

Two-sex demography, sexual niche differentiation, and the geographic range limits of Texas bluegrass (*Poa* *arachnifera*)

Tom E.X. Miller^{1,*} and Aldo Compagnoni^{2,3}

The authors wish to be identified to the reviewers.

1. Program in Ecology and Evolutionary Biology, Department of BioSciences, Rice University, Houston, TX 77005; 2. Institute of Biology, Martin Luther University Halle-Wittenberg, Halle, Germany; 3. German Centre for Integrative Biodiversity Research (iDiv), Leipzig, Germany; * Corresponding author; e-mail: tom.miller@rice.edu

Manuscript elements: Figures 1–6, online appendices A–C. Figure 2 and Figure 6 are to print in color.

Keywords: demography; dioecy; intra-specific niche heterogeneity; matrix projection model; sex ratio; range limits.

Manuscript type: Article.

Prepared using the suggested L^AT_EX template for *Am. Nat.*

Abstract

1 Understanding the mechanisms that generate biogeographic range limits is a long-standing
2 goal of ecology. It is widely hypothesized that distributional limits reflect the envi-
3 ronmental niche, but this hypothesis is complicated by widespread potential for intra-
4 specific niche heterogeneity. In dioecious species, sexual niche differentiation may cause
5 divergence between the sexes in their limits of environmental suitability. We studied
6 range boundary formation in Texas bluegrass (*Poa arachnifera*), a perennial dioecious
7 plant, testing the alternative hypotheses that range limits reflect the niche limits of fe-
8 males only versus the combined contributions of females and males, including their
9 inter-dependence via mating. Common garden experiments across a longitudinal aridity
10 gradient revealed female-biased flowering approaching eastern range limits, suggesting
11 that mate limitation may constrain the species' distribution. However, a demographic
12 model showed that declines in λ approaching range limits were driven almost entirely
13 by female vital rates. The dominant role of females was attributable to seed viability
14 being robust to sex ratio variation and to low sensitivity of λ to reproductive transitions.
15 We suggest that female-dominant range limits may be common to long-lived species
16 with polygamous mating systems, and that female responses to environmental drivers
17 may often be sufficient for predicting range shifts in response to environmental change.

Keywords

18
19 demography; dioecy; intra-specific niche heterogeneity; matrix projection model; sex
20 ratio; range limits

21

Introduction

22 Understanding the processes that generate species' distributional limits is a foundational
23 objective of ecology. The niche concept is central to theory for range limits (Hutchinson,
24 1958) and available evidence suggests that geographic distributions may often be inter-
25 preted as ecological niches "writ large" (Hargreaves et al., 2013; Lee-Yaw et al., 2016).
26 Species distribution modeling has long capitalized on this idea to infer niche charac-
27 teristics from statistical associations between occurrence and environmental variables.
28 In contrast, there is growing interest in process-based models of range limits, where
29 individual-level demographic responses to environmental variation inform predictions
30 about the ecological niche and environmental limits of population viability (i.e., at least
31 replacement-level population growth, $\lambda \geq 1$) (Diez et al., 2014; Merow et al., 2017, 2014).
32 The mechanistic understanding offered by process-based models of range limits pro-
33 vides a potentially powerful vehicle for predicting range shifts in response to current
34 and future environmental change (Ehrlén and Morris, 2015; Evans et al., 2016).

35 The widespread idea that range limits reflect niche limits intersects awkwardly with
36 another pervasive concept in ecology: intra-specific niche heterogeneity. This refers to
37 the fact that individuals within a population or species may differ in their interactions
38 with the biotic and/or abiotic environment (Araújo et al., 2011; Bolnick et al., 2002; Holt,
39 2009). Intra-specific niche differences may correspond to demographic state variables
40 such as life stage, size class or other, unmeasured aspects of individual identity. If range
41 limits are a geographic manifestation of niche limits, but a single population or species
42 may be comprised of many niches, then whose niche is it that determines the geographic
43 distribution and how would we know?

44 Sexual niche differentiation is a common form of intra-specific niche heterogeneity
45 (Bolnick et al., 2002) and has been widely documented in animals (the vast majority
46 of which are dioecious) and plants (ca. 6% of angiosperms are dioecious: Renner and
47 Ricklefs 1995). The prevalence of sexual niche differentiation was recognized by Darwin
48 (1871), who described “different habits of life, not related...to the reproductive functions”
49 of females and males. There are now many examples of sex differences in trophic posi-
50 tion (Law and Mehta, 2018; Pekár et al., 2011), habitat use (Bowyer, 2004; De Lisle et al.,
51 2018; Phillips et al., 2004), and responses to climate (Gianuca et al., 2019; Petry et al.,
52 2016; Rozas et al., 2009), differences that may or may not be accompanied by sexual
53 dimorphism. It has been hypothesized that sexual niche differentiation may evolve by
54 natural selection when it reduces competitive or other antagonistic interactions between
55 the sexes (Bolnick and Doebeli, 2003; De Lisle and Rowe, 2015), as a byproduct of nat-
56 urally or sexually selected size dimorphism (Shine, 1989; Temeles et al., 2010), or when
57 females and males pay different costs of reproduction (Bierzychudek and Eckhart, 1988).

58 Sexual niche differentiation can translate to sex-specific advantages in different envi-
59 ronments, causing skew in the operational sex ratio (OSR: relative abundance of females
60 and males available for mating) even if the primary (birth) sex ratio is unbiased (Eberhart-
61 Phillips et al., 2017; Shelton, 2010; Veran and Beissinger, 2009). Indeed, environmental
62 clines in OSR have been widely documented in plants and animals at fine spatial scales
63 (Bertiller et al., 2002; Bisang et al., 2020; Eppley, 2001; Groen et al., 2010; Hultine et al.,
64 2018) as well as broader climatic clines across alititudtes or latitudes (Caruso and Case,
65 2007; Dudaniec et al., 2021; Ketterson and Nolan Jr, 1976; Petry et al., 2016). At range
66 margins, where environments are extreme relative to the range core, demographic dif-
67 ferences between the sexes, and hence skew in the OSR, may be greatest. In dioecious

68 plants, for example, populations at upper altitudes and latitudes and in the more xeric
69 margins of species' ranges tend to be male-biased (Field et al., 2013b).

70 Returning to the question of whose niche determines range limits given the potential
71 for sexual niche differentiation, classic ecological theory assumes the answer. "Female
72 dominance" is a pervasive, often implicit feature of population-dynamic models whereby
73 male availability is assumed to have no influence on female fertility (Caswell and Weeks,
74 1986; Miller and Inouye, 2011; Rankin and Kokko, 2007). This assumption is wrong,
75 of course, but it may be *adequate* when the sex ratio is balanced or exhibits little varia-
76 tion. The female-dominant perspective predicts that female responses to environmental
77 variation should govern range limits (Fig. 1). However, females may be mate-limited
78 in environments in which they are favored, which could reduce population viability in
79 marginal environments. This creates an additional, "two-sex" pathway by which envi-
80 ronmental drivers may set distributional limits, via perturbations to the mating pool that
81 arise from sex-specific responses to the environment (Fig. 1).

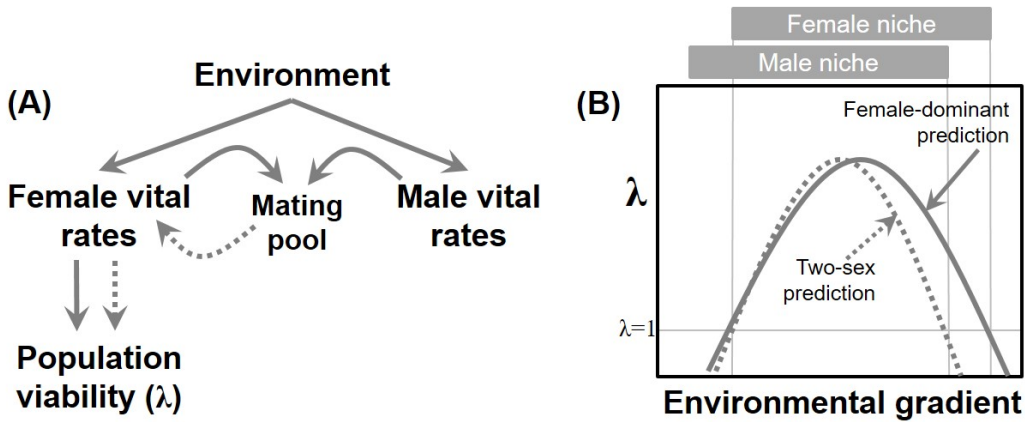


Figure 1: Hypotheses for how environmental variation can affect population viability and range limits in dieocious species. Under the female-dominant hypothesis, environmental drivers affect population growth (λ) through effects on females, alone (A). In geographic / environmental space, this translates to range boundaries that arise at the limits of the female environmental niche, irrespective of where they fall with respect to the male niche (B). Under the two-sex hypothesis, environmental drivers can affect λ through sex-specific responses, which may skew the sex ratio of the mating pool and feed back to affect female fertility via mate availability (A). In this case, expectations for range limits may differ from the female-dominant prediction, since mate limitation in environments that favor females over males may reduce population viability (B). These are alternative hypotheses in the strict sense, but as the role of males becomes weaker the two-sex prediction converges on the female-dominant prediction.

82 Here we ask whether female demographic responses to environmental variation,
 83 alone, are sufficient to understand the ecological origins of range limits, or whether
 84 males and female-male interactions must additionally be considered. As an experimen-
 85 tal model, we worked with a dieocious plant species (Texas bluegrass [*Poa arachnifera*])
 86 narrowly distributed across the sharp longitudinal aridity gradient of the southern Great
 87 Plains, US (Fig. 2). We hypothesized that sexual niche differentiation with respect to lon-
 88 gitudinal variation in aridity may lead to skewed sex ratios approaching range limits,
 89 and that mate limitation at environmental extremes could cause range boundaries to

90 deviate from female-dominant expectations.

91 This study was conducted in four parts. First, we conducted surveys to ask whether
92 natural populations of Texas bluegrass exhibit longitudinal clines in operational sex ra-
93 tio across the aridity gradient. Second, we conducted a common garden experiment at
94 14 sites throughout the southern Great Plains to quantify sex-specific demography in
95 variable abiotic environments. Third, we conducted a local sex ratio manipulation ex-
96 periment to quantify how viable seed production by females responds to variation in
97 OSR. Finally, we connected sex-specific demography with inter-sexual mating dynam-
98 ics in a two-sex modeling framework to derive demographically-driven predictions for
99 geographic limits of population viability ($\lambda \geq 1$). We analyzed the demographic model
100 to decompose the decline in λ approaching range limits into contributions from female-
101 dominant and two-sex pathways (Fig. 1).

102 **Materials and methods**

103 *Study system and natural population surveys*

104 *Poa arachnifera* (Texas bluegrass) is a perennial, cool-season (C3) grass endemic to the
105 southern Great Plains. This species occurs almost exclusively in central Texas, Okla-
106 homa, and southern Kansas (Fig. 2) though there are occasional records of adventive
107 populations in other U.S. states¹. Like all grasses, *P. arachnifera* is wind-pollinated. In-
108 dividuals can be sexed only when flowering, in early spring, based on the presence of
109 stigmas (females) or anthers (males) in the inflorescence. Following inflorescence and
110 seed production, plants go dormant for the hot summer months and vegetative growth

¹<http://bonap.net/Napa/TaxonMaps/Genus/County/Poa>

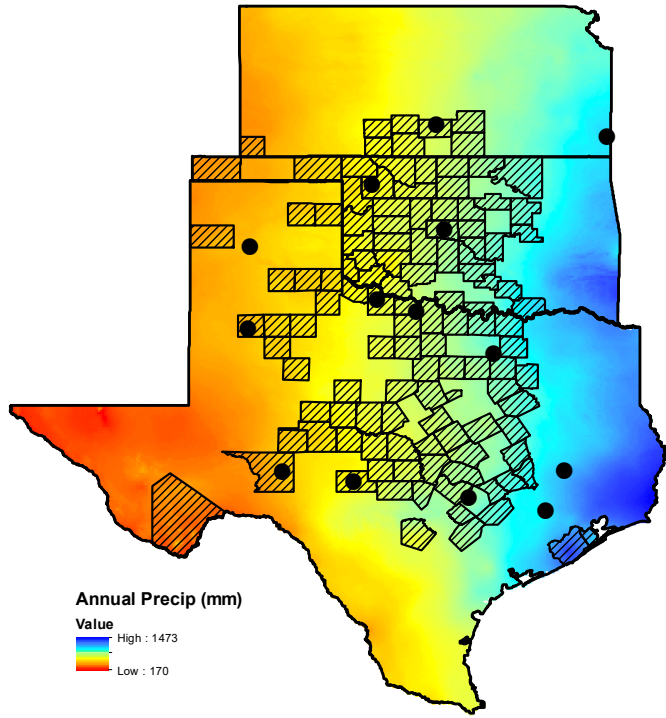


Figure 2: Geographic and environmental distribution of *P. arachnifera* in Texas, Oklahoma, and Kansas. Hatched shapes show counties with herbarium records of occurrence. Color shows geographic variation in annual precipitation (mm) based on 30-year normals from WorldClim (Fick and Hijmans, 2017). Points show sites for the common garden transplant experiment.

111 resumes in fall. Individuals grow via rhizomes to form patches that may be as large as
 112 $50m^2$ in area. Sex in *P. arachnifera* is genetically based (Renganayaki et al., 2005, 2001)
 113 and the primary sex ratio is 1:1 (J. Goldman, USDA-ARS, *unpubl. data*). The rhizomatous
 114 growth habit allowed us to clonally propagate large numbers of known-sex individuals
 115 for experiments, as we describe below.

116 We surveyed *P. arachnifera* across its range to establish whether natural populations
 117 exhibited geographic clines in OSR corresponding to the longitudinal aridity gradient.

118 We visited 14 populations in spring 2012 and 8 in spring 2013 (Table A1). At each loca-
119 tion, we searched for *P. arachnifera* along roads, trails, or creek drainages and recorded
120 the number of female and male patches that we encountered and the number of inflores-
121 cences in each patch. To quantify the mating environment, we focus our analyses on the
122 sex ratio of inflorescences rather than patches, since a single patch makes different con-
123 tributions to the mating pool depending on whether it has few or many inflorescences.

124 *Statistical analysis of natural population surveys*

125 We fit a binomial generalized linear model (glm), where “successes” were female in-
126 florescences and “trials” were total inflorescences, to test whether the OSR varied sys-
127 tematically with respect to longitude. Here and in the experiments that follow we use
128 longitude as a proxy variable that captures all east-west environmental variation, notably
129 precipitation (Fig. 2) but also factors that co-vary with precipitation such as productivity.
130 This statistical model and all those that follow were fit in a Bayesian statistical framework
131 using Stan (Carpenter et al., 2017) and R package ‘rstan’ (Stan Development Team, 2020)
132 with vague priors on all parameters. In all cases, model fit was assessed with poste-
133 rior predictive checks (Gelman et al., 1996). All code for statistical and demographic
134 modeling is available at <https://github.com/texmiller/POAR-range-limits>.

135 *Common garden experiment*

136 *Source material and experimental design*

137 We established a common garden experiment at 14 sites throughout and beyond the
138 geographic distribution of *P. arachnifera* (Fig. 2, Table A2). Experimental sites spanned

¹³⁹ latitudinal and longitudinal variation, though we focus here on longitude. During the
¹⁴⁰ three years of this experiment (2014–2017), total precipitation at each site closely tracked
¹⁴¹ longitude (Fig. A1), as expected based on longer-term climate trends (Fig. 2). Source
¹⁴² material for the experiment came from 8 sites, which were a subset of the sites that
¹⁴³ were visited for the natural population survey (Table A1). At these sites, we collected
¹⁴⁴ vegetative tillers from flowering individuals of each sex (mean: 11.6 individuals per
¹⁴⁵ site, range: 2–18). These were brought back to the Rice University greenhouse, where
¹⁴⁶ they were clonally propagated in ProMix potting soil and supplemented with Osmocote
¹⁴⁷ slow-release fertilizer at 78–80°F under natural humidity and light.

¹⁴⁸ Common gardens were set up in Fall (October–December) 2014. At each site, we es-
¹⁴⁹ tablished 14 experimental blocks, which corresponded to a tree or woodland edge, pro-
¹⁵⁰ viding partial shade that mimics this species' natural micro-environment. We planted
¹⁵¹ 3 females and 3 males in each block, for a total of 42 individuals per sex per site and
¹⁵² 1176 total plants across sites, with all source collections represented at all sites. Indi-
¹⁵³ viduals were spaced within blocks to allow space for rhizomatous growth that could be
¹⁵⁴ clearly attributed to individual transplants. To promote establishment, we cleared vege-
¹⁵⁵ tation immediately surrounding transplants and provided ca. 1 L of water at the time of
¹⁵⁶ transplanting but provided no subsequent watering, fertilization, or competitor removal.

¹⁵⁷ We visited each site during May of 2015, 2016, and 2017. For each individual in each
¹⁵⁸ year, we recorded data for four demographic vital rates: survival status (alive or dead),
¹⁵⁹ size (number of tillers and patch area), flowering status (reproductive or vegetative), the
¹⁶⁰ number of panicles produced by flowering plants.

161 *Statistical analysis of common garden experiment*

162 We analyzed the demographic vital rates with generalized linear mixed models in a
163 hierarchical Bayesian framework. All the vital rates shared a common linear predictor for
164 the expected value that included fixed effects of size, sex, linear and quadratic terms for
165 longitude, and all 2- and 3-way interactions. We included quadratic effects of longitude
166 to account for the possibility of non-monotonic responses, following the hypothesis that
167 fitness may peak in the center of the range. The linear predictor also included random
168 effects of site, block, and source population of the transplant. We pooled all three years
169 of observations for analysis so we did not explicitly model temporal variation but our
170 results are implicitly averaged over years.

171 The survival and flowering data were Bernoulli distributed, and these models applied
172 the logit link function. We modeled panicle counts as zero-truncated negative binomial
173 using the log link. For growth, we modeled tiller number with a zero-truncated Poisson-
174 Inverse Gaussian (PIG) distribution. For flowering and panicle production in year t , the
175 size covariate was the natural logarithm of tiller number in year t . For survival and
176 size in year t , the size covariate was the natural logarithm of tiller number in year $t - 1$
177 (for 2015 data, size in year $t - 1$ was transplant size at the time of planting). Posterior
178 predictive checks indicated that these models described the data well (Fig. B1).

179 *Sex ratio experiment*

180 At one site near the center of the range (Lake Lewisville Environmental Learning Area,
181 Texas), we established a separate experiment to quantify how sex ratio variation affects
182 female reproductive success. Details of this experiment, which was conducted in 2014–

183 2015, are described in Compagnoni et al. 2017. Briefly, we established 124 experimental
184 populations in $0.4m \times 0.4m$ plots that varied in population density (1–48 plants/plot) and
185 sex ratio (0–100% female), with 2–4 replicates for each of 34 density-sex ratio combina-
186 tions. The experiment was established ca. 1 km from a natural population at this site and
187 plots were situated with a minimum of 15 m spacing, a buffer that was intended to limit
188 pollen movement between plots (pilot data indicated that $\geq 90\%$ of wind pollination oc-
189 curred within 13m). We measured female reproductive success in different density and
190 sex ratio environments by collecting panicles from a subset of females in each plot at the
191 end of the reproductive season. In the lab, we counted the total number of seeds on each
192 panicle and assessed seed viability in the greenhouse with germination trials of 25 seeds
193 per panicle. We also conducted tetrazolium-based seed viability assays (17–57 seeds per
194 panicle, mode: 30).

195 *Statistical analysis of sex ratio experiment*

196 Our previous study examined how interactions between density and frequency (sex ra-
197 tio) dependence contributed to female reproductive success (Compagnoni et al., 2017).
198 Here we focus solely on sex ratio variation, averaging over variation in density. Our goal
199 was to estimate a ‘mating function’ that defines how availability of male panicles affects
200 the viability of seeds on female panicles. We modeled the seed viability data with a
201 binomial distribution where the probability of viability (v) was given by:

$$v = v_0 * (1 - OSR^\alpha) \quad (1)$$

202 where OSR is the operational sex ratio (fraction of panicles that were female) in our

203 experimental populations. This function has the properties, supported by our previous
204 work (Compagnoni et al., 2017), that seed viability is maximized at v_0 as OSR approaches
205 zero (strongly male-biased) and goes to zero as OSR approaches 1 (strongly female-
206 biased). Parameter α controls how viability declines with increasing female bias.

207 We modeled germination data from greenhouse trials similarly, where counts of ger-
208 minants were modeled as binomial successes. Since germination was conditional on seed
209 viability, the probability of success was given by the product $v * g$, where v is a function
210 of OSR (Eq. 1) and g is assumed to be constant. The germination trials alone do not
211 provide enough information to independently estimate v and g but the combination of
212 viability and germination data allowed us to do so. For both viability and germination,
213 we found that accounting for overdispersion with a beta-binomial response distribution
214 improved model fit.

215 *Demographic model of range limits*

216 The statistical models for the common garden and sex ratio experiments provided the
217 backbone of the full demographic model, a matrix projection model (MPM) structured
218 by size (tiller number) and sex. Following the statistical modeling, the MPM accommo-
219 dates longitude as a predictor variable, allowing us to identify the longitudinal limits of
220 population viability ($\lambda \geq 1$) and investigate the underlying drivers of population decline
221 at range limits.

222 For a given longitude, let $F_{x,t}$ and $M_{x,t}$ be the number of female and male plants of
223 size x in year t , where $x \in \{1, 2, \dots, U\}$ and U is the maximum number of tillers a plant can
224 attain (set to the 99th percentile of observed maximum size). We also include additional
225 state variables for new recruits, F_t^R and M_t^R , which we assume do not reproduce in their

226 first year. For ease of presentation, we do not symbolically show longitude effects in the
 227 vital rate functions for growth, survival, flowering, and panicle production but these all
 228 included longitude effects on the intercept and slope (with respect to size) as a second-
 229 order polynomial, following the statistical models. We assume that the parameters of sex
 230 ratio-dependent mating (Eq. 1) do not vary with longitude.

231 For a pre-breeding census, the expected numbers of recruits in year $t + 1$ is given by:

$$F_{t+1}^R = \sum_{x=1}^U [p^F(x) \cdot c^F(x) \cdot d \cdot v(\mathbf{F}_t, \mathbf{M}_t) \cdot m \cdot \rho] F_{x,t} \quad (2)$$

$$M_{t+1}^R = \sum_{x=1}^U [p^F(x) \cdot c^F(x) \cdot d \cdot v(\mathbf{F}_t, \mathbf{M}_t) \cdot m \cdot (1 - \rho)] F_{x,t} \quad (3)$$

232 where p^F and c^F are flowering probability and panicle production for females of size x , d
 233 is the number of seeds (fertilized or unfertilized) per female panicle, v is the probability
 234 that a seed is fertilized, m is the probability that a fertilized seed germinates, and ρ is
 235 the primary sex ratio (proportion of recruits that are female). Seed fertilization depends
 236 on the OSR of panicles (following Eq. 1) which was derived from the $U \times 1$ vectors of
 237 population structure \mathbf{F}_t and \mathbf{M}_t :

$$v(\mathbf{F}_t, \mathbf{M}_t) = v_0 * \left[1 - \left(\frac{\sum_{x=1}^U p^F(x)c^F(x)F_{x,t}}{\sum_{x=1}^U p^F(x)c^F(x)F_{x,t} + p^M(x)c^M(x)M_{x,t}} \right)^\alpha \right] \quad (4)$$

238 Finally, the dynamics of the size-structured component of the population are given
 239 by:

$$F_{y,t+1} = [\sigma \cdot g^F(y, x=1)] F_t^R + \sum_{x=1}^U [s^F(x) \cdot g^F(y, x)] F_{x,t} \quad (5)$$

$$M_{y,t+1} = [\sigma \cdot g^M(y, x=1)] M_t^R + \sum_{x=1}^U [s^M(x) \cdot g^M(y, x)] M_{x,t} \quad (6)$$

240 For both females and males, the first term represents seedlings that survived their first
 241 year and enter the size distribution of established plants. Because our common gar-
 242 den experiment relied on greenhouse-raised transplants, we had little information on
 243 these early life cycle transitions. We used the seedling survival probability (σ) from our
 244 demographic studies of the hermaphroditic, perennial congener *Poa autumnalis* in east
 245 Texas (T.E.X. Miller and J.A. Rudgers, *unpublished data*) as a stand-in for *P. arachnifera*,
 246 and we assume this probability was constant across sexes and longitudes (posterior
 247 mean $\sigma = 0.09$). We also assume that surviving seedlings reach size y with probabil-
 248 ity $g(y, x=1)$, the expected future size of 1-tiller plants from the transplant experiment.
 249 The second term represents survival and size transition of established plants from the
 250 previous year, where s and g give the probabilities of surviving at size x and growing
 251 from sizes x to y , respectively, and superscripts indicate that these functions may be
 252 unique to females (F) and males (M).

253 Because the two-sex MPM is nonlinear (vital rates affect and are affected by popu-
 254 lation structure) we estimated the asymptotic geometric growth rate (λ) by numerical
 255 simulation, and repeated this across a range of longitudes. We used a regression-style
 256 Life Table Response Experiment (Caswell, 2001) to decompose the change in λ towards
 257 range limits into contributions from female and male vital rates (the female-dominant
 258 hypothesis predicts that declines in λ at range limits are driven solely by females). The

259 LTRE approximates the change in λ with longitude as the product of the sensitivity of λ
260 to the parameters times the sensitivity of the parameters to longitude, summed over all
261 parameters:

$$\frac{\partial \lambda}{\partial \text{Longitude}} \approx \sum_i \frac{\partial \lambda}{\partial \theta_i^F} \frac{\partial \theta_i^F}{\partial \text{Longitude}} + \frac{\partial \lambda}{\partial \theta_i^M} \frac{\partial \theta_i^M}{\partial \text{Longitude}} \quad (7)$$

262 Here, θ_i^F and θ_i^M represent sex-specific parameters: the regression coefficients for the
263 intercepts and slopes of size-dependent vital rate functions. Because LTRE contributions
264 are additive, we summed across vital rates to compare the total contributions of female
265 and male parameters. Finally, we compared the two-sex MPM to the corresponding
266 female-dominant model (Fig. 1B) by setting $v(\mathbf{F}_t, \mathbf{M}_t) = v_0$, which decouples female
267 fertility from the composition of the mating pool.

268 Results

269 Sex ratio variation in natural populations

270 We found wide variation in operational sex ratio (proportion of total panicles that were
271 female) across 22 natural populations of *P. arachnifera*, including female-only and male-
272 only populations (Fig. 3A). There was a longitudinal trend to sex ratio variation, with
273 male-biased panicle production in the western parts of the range and female-biased pan-
274 icle production in the east.

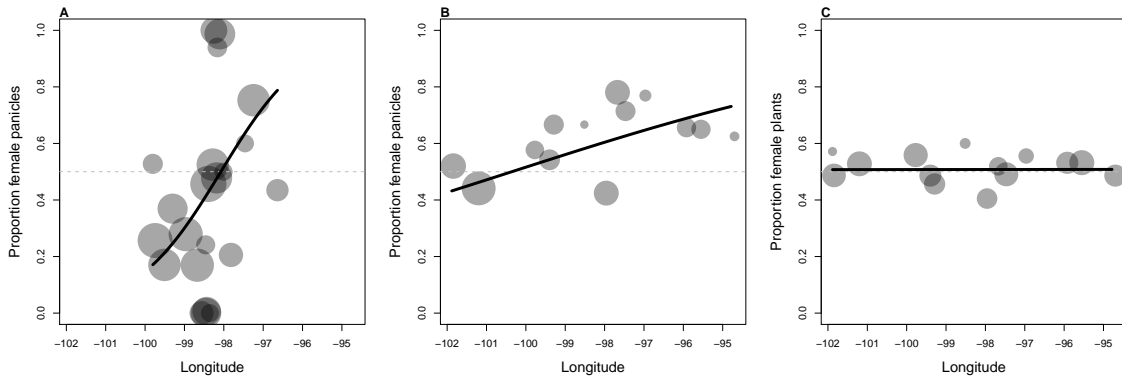


Figure 3: Sex ratio variation of *P. arachnifera* across its longitudinal distribution. **A**, Operational sex ratio (fraction of panicles that were female) in 22 natural populations; **B**, Operational sex ratio and **C**, sex ratio (fraction of plants that were female) in 14 common gardens. Within panels, point size is proportional to sample size (total number of panicles in **A,B** and total plants in **C**) as follows: **A**, min: 45, max: 2148; **B**, min: 1, max: 1021; **C**, min: 2, max: 79. In **B,C**, data are pooled across years. Lines show fitted binomial GLMs.

275

Geographic variation in sex-specific demography

276 In year one, there was near-total mortality of transplants at three sites in the common
 277 garden experiment due to various catastrophes (a flood, a drought, a pack of voles);
 278 otherwise, there was high (95%) establishment. There was strong longitudinal variation
 279 in demography, including sex-specific demographic responses that varied across vital
 280 rates and interactions between size, sex, and longitude. Where sex-specific demographic
 281 responses occurred, they were almost always in favor of females. In Fig. 4, we show
 282 binned means of raw data and fitted vital rate models for four vital rates (rows) and
 283 three size classes (columns); size was discretized for visualization only. This figure also
 284 shows the posterior distributions for the difference between the sexes across longitudes.

285 Annual survival probability was predicted to peak at western and eastern range

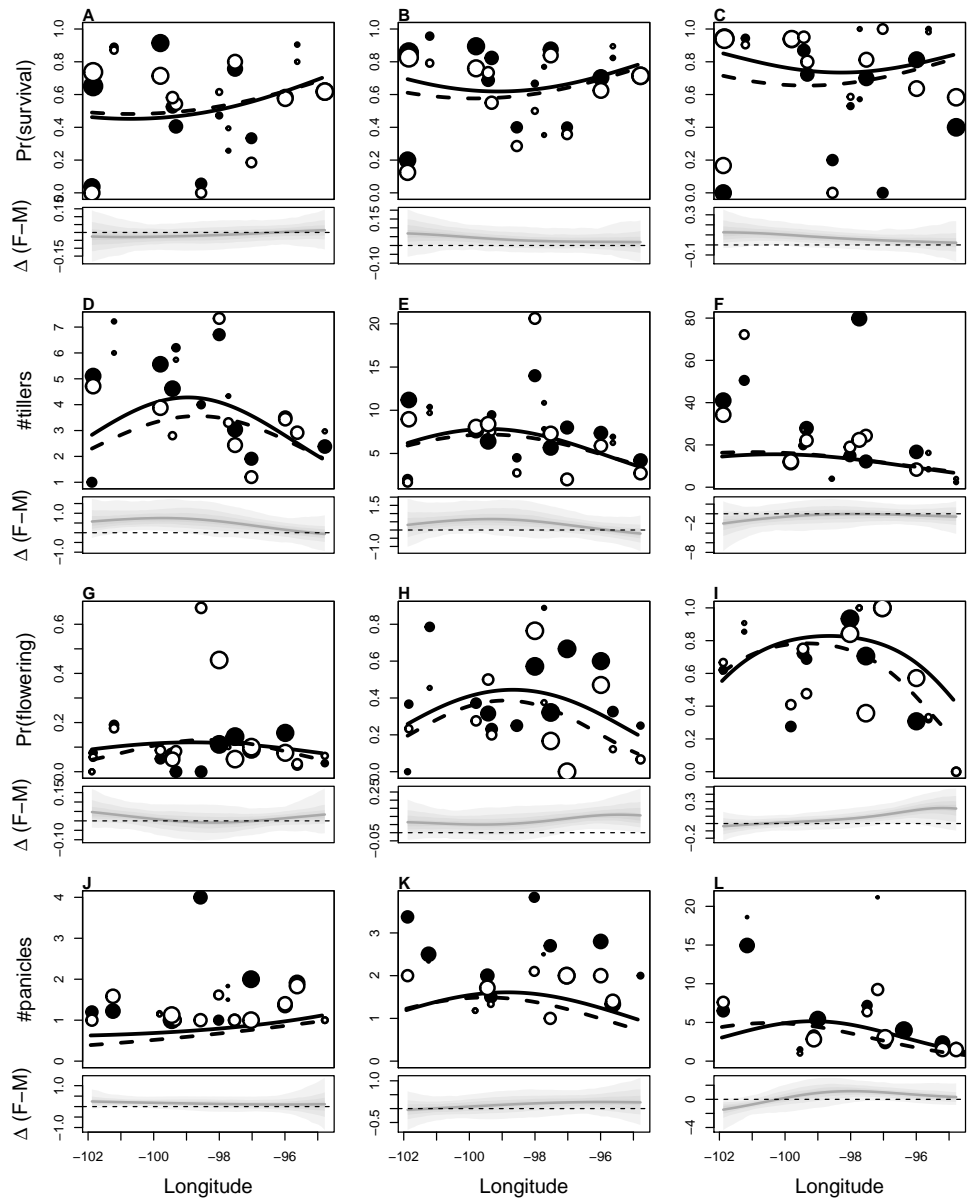


Figure 4: Sex-, size-, and longitude-related variation in: A–C, inter-annual probability of survival; D–F, inter-annual growth (change in number of tillers); G–I, probability of flowering; J–L, number of panicles produced given flowering. Points show means by site for females (filled) and males (open) and small (left column), medium (middle column), and large (right column) size classes (discretized, for visualization only). Point size is proportional to the sample size of the mean. Lines show fitted statistical models for females (solid) and males (dashed) based on posterior mean parameter values. Lower panels below each data panel show the posterior distribution of the difference between females and males as a function of longitude (positive and negative values indicate female and male advantage, respectively); dashed horizontal line shows zero difference.

edges and was lowest at intermediate longitudes (Fig. 4A-C). There was a modest female survival advantage but only at the western range edge for large sizes. Other vital rates showed the opposite (and more expected) longitudinal pattern for most sizes, with peaks in the center of the range and declines at eastern and western edges. There was a female growth advantage for small sizes at western longitudes (Fig. 4D-F). The strongest sex difference was in the probability of flowering: females had a flowering advantage, especially for large sizes and at eastern longitudes (Fig. 4G-I). Finally, panicle production by flowering plants was similar between the sexes for most sizes, though for the largest sizes there were advantages for males in the west and females in the east (Fig. 4J-L).

Sex differences in flowering and panicle production generated a longitudinal trend in the operational sex ratio of our common garden populations consistent with (but weaker than) the trend in natural populations: the fraction of total panicles that were female in our common gardens increased from west to east (Fig. 3B) even as the fraction of surviving plants that were female did not show a longitudinal trend (Fig. 3C). Thus, in recapitulating the natural OSR pattern, the common garden experiment revealed that the longitudinal trend in the mating pool of natural populations was due to the reproductive niche of females extending farther east than that of males, and not to sex differences in mortality.

Sex-ratio dependent seed fertilization

Seed fertilization by females declined with increasing female bias in the sex ratio manipulation experiment. Fertilization success was greatest for females that were rare in male-biased populations, where 75-80% of initiated seeds were viable (Fig. 5). Fertilization was robust to sex ratio variation until ca. 75% of the panicles in a population were

309 female, at which point fertilization strongly declined due to pollen limitation. The fitted
 310 model specifies that seed fertilization goes to zero as female bias goes to 100% (Eq. 1),
 311 and this assumption was generally consistent with the experimental results, where the
 312 majority (63%) of females from female-only populations produced zero viable seeds. The
 313 occasional production of viable seeds in female-only populations (Fig. 5) likely reflects
 314 rare pollen contamination between experimental plots.

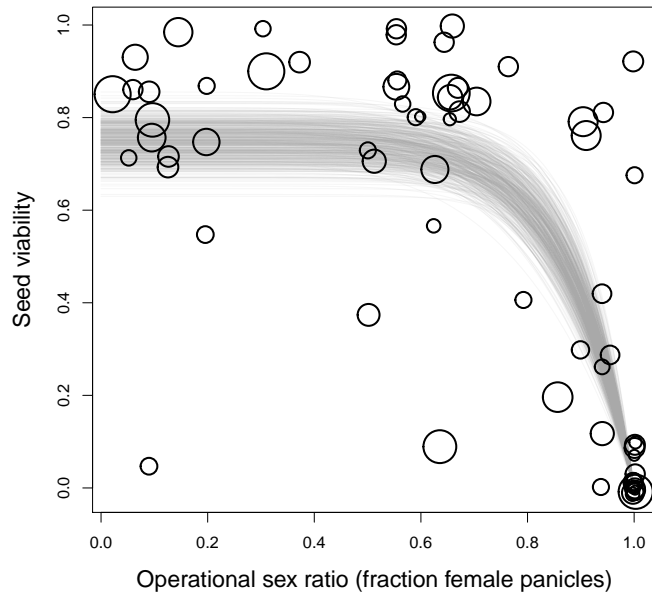


Figure 5: Seed fertilization success in relation to operational sex ratio (fraction of panicles that are female) in experimental populations. Circles show data from tetrazolium assays of seed viability; circle size is proportional to the number of seeds tested (min: 14, max: 57). Lines show model predictions (Eq. 1) for 500 samples from the posterior distribution of parameter estimates.

315

Two-sex model of range limits

316 The process-based demographic model connected sex-specific vital rate responses to
317 longitudinal variation (Fig. 4) with sex ratio-dependent mating (Fig. 5) to predict the
318 contributions of females and males to range limitation. The model predicted maxi-
319 mum fitness in the center of the range and loss of population viability at longitudes
320 that corresponded well with observed range limits. Specifically, the western-most and
321 eastern-most county records of *P. arachnifera* fell within the uncertainty distribution of
322 the model's predictions (represented by the shading in Fig. 6A), bolstering our confi-
323 dence that the model effectively captured the demographic drivers of range limitation in
324 this species. Also, the asymptotic population structure predicted by the model showed
325 female bias in the operational (panicle) sex ratio toward the eastern range margins, con-
326 sistent with observations from the common garden and natural populations (Fig. B4A).
327 Female bias in the OSR was predicted to cause declines in seed viability toward eastern
328 range margins (Fig. B4B). However, this effect was weak in magnitude because predicted
329 OSR bias was not extreme enough to cause strong declines in viability, given the re-
330 lationship derived from the sex ratio manipulation experiment (Fig. 5). Furthermore,
331 population viability at the eastern range margin was weakly sensitive to seed viability
332 relative to other vital rates (B4C). These observations underscore the next set of results.

333 LTRE decomposition revealed that declines in λ approaching range limits were driven
334 almost exclusively by females (Fig. 6B) with near-zero contributions from males (Fig.
335 6C). Thus, range limitation was an effectively female-dominant process, despite system-
336 atic geographic variation in sex ratio. Correspondingly, predictions of the two-sex model
337 were nearly indistinguishable from a corresponding female-dominant model with all else

338 equal, with only very modest differences in predictions of the two models emerging in
339 the eastern part of the range (Fig. B3).

340 Decomposition analysis further revealed that multiple female vital rates contributed
341 to range limits, some in opposing directions. Because female survival increased toward
342 range limits (Fig 4A-C), this vital rate had a contribution to $\frac{\partial \lambda}{\partial \text{Longitude}}$ that was opposite
343 in sign to the other vital rates (Fig. 6B). However, increased survival at range edges was
344 not sufficient to offset declines in other vital rates. The overall decline in λ was driven
345 most strongly by a combination of reduced flowering and growth in females at both the
346 eastern and western limits (Fig. 6B).

347 Skew in the OSR predicted by the demographic model was less extreme than was
348 observed in natural and experimental populations (B4A). This occurred because sex dif-
349 ferences in demography, especially flowering, were most pronounced at the largest sizes,
350 and the MPM predicted that these sizes were very rare at stable population structure.
351 The stable size distribution predicted by the MPM corresponded well to the common
352 garden data (from which the MPM was built) but was much smaller, on average, than
353 the size distribution we observed in natural populations (Fig. C2), presumably because
354 transplants did not grow like “real” plants and/or did not have time in our three-year
355 experiment to reach those sizes. In Appendix C, we explore whether higher growth
356 rates, leading to a more realistic size distribution, would lead to a more important role
357 for males. In numerical experiments with growth parameters, we found that larger size
358 distributions led to stronger female bias and thus stronger reductions in seed viability
359 at eastern range margins (Fig. C3). While these changes increased the contributions of
360 males to range limitation, female contributions were still more than twice as important as
361 males, and there was very little difference between predictions of the two-sex and female-

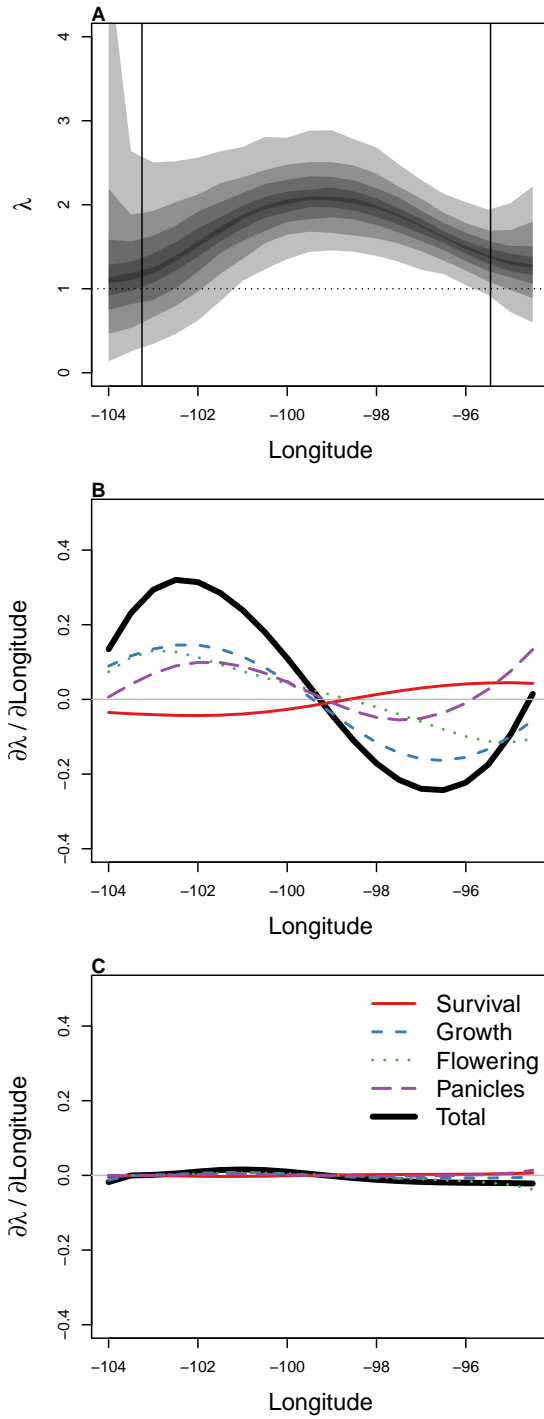


Figure 6: Population growth (λ) as a function of longitude, predicted by the two-sex MPM that incorporates sex-specific demographic responses to longitude with sex ratio-dependent seed fertilization. A, posterior distribution of λ , where shaded regions show the 25, 50, 75, and 95% percentiles of parameter uncertainty. Dashed horizontal line indicates the limit of population viability ($\lambda = 1$) and vertical lines show the longitudes of Brewster and Brazoria Counties, TX, the western- and eastern-most occurrence records of *P. arachnifera*. B–C, LTRE decomposition of the sensitivity of λ to longitude into additive vital rate contributions of females (B) and males (C) based on posterior mean parameter estimates.

362 dominant models even under this elevated growth scenario (Fig. C4). This leads us to
363 conclude that, while our common garden-parameterized model may quantitatively un-
364 derestimate OSR bias and its demographic consequences relative to natural populations,
365 our qualitative conclusion that range boundary formation is effectively female-dominant
366 in this system is robust to any biases imposed by the growth trajectories and size distri-
367 butions of common garden populations.

368

Discussion

369 Understanding the causes of decline in population viability at range edges is a classic
370 ecological problem and the foundation for predicting how species' ranges will respond
371 to global change drivers. Sexual niche differentiation has the potential to generate skew
372 in the mating pool across environmental gradients and may therefore contribute to re-
373 productive failure at range edges of dioecious species. In Texas bluegrass, we found
374 evidence for sexual niche differentiation that manifested over a large-scale geographic
375 gradient: the female reproductive niche (environment-dependent flowering and panicle
376 production) extended farther east than that of males, generating female-biased opera-
377 tional sex ratios toward the eastern, mesic range margins, a pattern detected in natural
378 populations and recapitulated in our common garden populations. Furthermore, seed
379 viability declined with increasing skew in the OSR, indicating that mate (pollen) limita-
380 tion can limit the reproductive output of female-biased mating pools. It would appear
381 that all the pieces are in place for an important role of two-sex dynamics in contributing
382 to distributional limits of Texas bluegrass, particularly at the eastern range edge. Yet,
383 insights derived from the field-parameterized population model indicate the opposite:
384 range limitation in this species is an effectively female-dominant process, with negligible

385 contributions from males. Thus, in this system and likely others, female dominance is
386 an adequate framework for understanding range dynamics: despite evidence for sexual
387 niche differentiation, only the female niche mattered for determining the environmental
388 limits of population viability. This does not mean that sex is unimportant, but rather that
389 lack of sex is never so severe that it limits population viability.

390 The limited role of males in our experimental system can be explained by two factors.
391 First, seed fertilization was robust to variation in OSR and was not predicted to strongly
392 decline within the range of OSR bias that we observed and modeled, suggesting that few
393 males are required to pollinate all or most females. Second, population growth (λ) was
394 weakly sensitive to seed viability, which further buffered the demographic consequences
395 of sex ratio bias. We speculate that our qualitative conclusions should apply to other
396 species or systems that satisfy either, but especially both, of these conditions. While
397 there are striking examples of female-biased sex ratios causing declines in population
398 growth (Milner-Gulland et al., 2003) or range expansion (Miller and Inouye, 2013), other
399 examples suggest limited demographic consequences of sex ratio variation (Ewen et al.,
400 2011; Gownaris et al., 2020; Mysterud et al., 2002). Ultimately, sensitivity of female repro-
401 ductive success to sex ratio should depend strongly on the mating system, with female
402 dominance at the “extremely polygamous” end of a continuum (Miller et al., 2011). The
403 sensitivity of population viability to female reproductive success, in turn, is likely pre-
404 dicted by life history strategy: in long-lived, iteroparous species, population growth rates
405 are often weakly sensitive to reproduction relative to growth and survival (Franco and
406 Silvertown, 2004). We therefore hypothesize that range limits are more likely to be dom-
407 inated by the female environmental niche in longer-lived species with more polygamous
408 mating systems, while males are more likely to play an important role in shorter-lived,

⁴⁰⁹ monogamous species that may be particularly sensitive to missed mating opportunities.
⁴¹⁰ As studies of sex ratio variation and sex-specific demography across species' ranges ac-
⁴¹¹ cumulate in the literature (e.g., Dudaniec et al., 2021; Lynch et al., 2014; Petry et al., 2016),
⁴¹² this hypothesis may be tractably pursued with comparative analyses.

⁴¹³ While life history and mating system may determine the demographic consequences
⁴¹⁴ of skewed sex ratios, the sensitivity of sex ratio to environmental drivers is another crit-
⁴¹⁵ ical ingredient of how environmental variation can affect the population dynamics of
⁴¹⁶ dioecious species. Our study adds to a growing body of work quantifying the demo-
⁴¹⁷ graphic mechanisms giving rise to skewed operational sex ratios using two-sex models
⁴¹⁸ (Eberhart-Phillips et al., 2017; Shelton, 2010; Veran and Beissinger, 2009) and parsing the
⁴¹⁹ contributions of environmental drivers (Bialic-Murphy et al., 2020). However, as a field,
⁴²⁰ we lack a strong predictive framework for how often and in which direction environ-
⁴²¹ mental drivers are likely to skew the operational sex ratio – and this gap is particularly
⁴²² important in the context of global change. We have focused on the limits of population
⁴²³ viability with respect to geographic environmental variation but analogous processes
⁴²⁴ will likely govern how populations respond to temporal environmental change (e.g., cli-
⁴²⁵ mate change), including direct effects on female demography and indirect effects via
⁴²⁶ perturbations to the mating pool (Fig. 1). There is a need to better understand and pre-
⁴²⁷ dict which species and types of species are susceptible to climate change-induced shifts
⁴²⁸ in OSR. Geographic variation in OSR may be an instructive proxy for how dioecious
⁴²⁹ species will respond to climate change (Petry et al., 2016). The link between OSR and
⁴³⁰ responses to climate adds value to studies of the causes and consequences of spatial vari-
⁴³¹ ation in sex ratio, particularly at geographic scales that encompass “past” and “future”
⁴³² conditions.

433 Previous studies of dioecious plants have shown that male bias is more common than
434 female bias and is particularly pronounced in harsh abiotic environments, likely reflect-
435 ing the greater resource requirements needed to pay the female cost of reproduction
436 (Bierzychudek and Eckhart, 1988; Field et al., 2013a,b). Our surveys of natural popula-
437 tions are consistent with the broader pattern of male-biased OSR at xeric range edges.
438 However, our common garden populations did not exhibit male bias in the xeric west –
439 averaged across years or in any single year (Fig. B2) – nor did we find any strong demo-
440 graphic evidence for a western male advantage (in fact, there was a western female ad-
441 vantage in growth and survival for some sizes). If male advantage / female disadvantage
442 under harsh abiotic conditions is driven by the greater resource requirements of females
443 then it is possible that clonal propagation and/or legacies of greenhouse rearing masked
444 the ‘true’ sex difference at xeric-edge common garden sites. Instead, the stronger pattern
445 of sex ratio bias was the female reproductive advantage at the mesic, eastern range edge.
446 We hypothesize that the mesic edge is limited by competition and that the female repro-
447 ductive advantage reflects competitive superiority of females, which has been suggested
448 in previous studies of Texas bluegrass (Compagnoni et al., 2017) and shown in other
449 dioecious plants (Eppley, 2006), particularly under mesic conditions (Chen et al., 2014).
450 Theory suggests that biotic interactions such as competition are likely to limit species'
451 ranges at the benign (e.g., mesic) end of abiotic gradients (Louthan et al., 2015) though
452 this has not been explored, to our knowledge, in the context of sex-structured dynamics.
453 Future studies in our system or others could test whether females and males differ in
454 their responses to biotic stressors at xeric and mesic range edges to reveal how biotic
455 factors shape range limits via sex-specific demography.

456 Beyond the novel elements of sex-structured demography and mate limitation, our

457 work informs and advances the broader literature on the processes generating species'
458 range limits in at least three ways. First, the Texas bluegrass case study demonstrates
459 that a process-based model capturing environment-dependent demography can accu-
460 rately predict geographic range limits: the predicted limits of $\lambda \geq 1$ corresponded well
461 to observed longitudinal limits from collection records, particularly given the uncer-
462 tainty characterized by our hierarchical Bayesian statistical approach. We parameterized
463 the model with respect to longitude, which tightly covaries with aridity in the southern
464 Great Plains. Extensions of this model that transition from implicit to explicit consid-
465 eration of aridity will allow us to forecast range responses of Texas bluegrass to future
466 climate change and ask whether climate change will reduce or amplify OSR bias and
467 mate limitation at longitudinal range edges. It would be interesting to additionally con-
468 sider this species' latitudinal limits, though our exploratory analyses revealed no clear
469 sex differences or sex ratio variation with respect to latitude.

470 Second, our results also provide novel evidence for contrasting demographic re-
471 sponses to environmental drivers throughout a species' range – or “demographic com-
472 pensation” (Doak and Morris, 2010; Villegas et al., 2015). Elevated performance in some
473 life history processes can compensate for declines in other processes and thus buffer
474 range-edge populations against harsh environmental conditions. In Texas bluegrass,
475 most vital rates declined toward eastern and western range limits but survival showed
476 the opposite pattern. Increased survival at longitudinal extremes partially offset declines
477 in other vital rates but this positive response was weaker than the negative responses.
478 Ultimately, increased survival was not sufficient to prevent declines in population vi-
479 ability from the range center to eastern and western limits, which were dominated by
480 declining female growth and flowering. A recent study found a similar pattern, where

481 compensation between vital rates could not prevent a decrease of population growth rate
482 towards the southern range edge of *Erythranthe cardinalis* (Sheth and Angert, 2018).

483 Third, our results highlight some important considerations in how environment-
484 dependent demographic models are best parameterized to derive insights into the drivers
485 of range limits. Our approach relied heavily on common garden populations, which
486 allowed us to plant and track known-sex individuals in contrasting environmental con-
487 ditions that encompass and exceed the natural geographic distribution. The ability to
488 robustly sample edge and beyond-edge environments is a powerful advantage of the
489 common garden transplant approach (Hargreaves et al., 2013). However, this also lim-
490 ited the size variation that we were able to include and model, and the size distributions
491 of common garden populations skewed consistently smaller than natural populations.
492 In Appendix C, we show that our conclusions are likely robust to this feature of the
493 common gardens. However, our ability to quantify the consequences of size representa-
494 tion is itself limited by size representation: we can simulate a population in which the
495 largest common garden sizes are more common than they actually were, but simulating
496 a population with sizes much larger than observed requires extrapolation of our statisti-
497 cal models, and we are skeptical about what insights such an exercise could provide (in
498 Appendix C, we extrapolated demographic performance to sizes 50% greater than the
499 observed maximum). This issue is not unique to our study but will be encountered by
500 any transplant study intended to yield inferences about range limits of species with sig-
501 nificant size structure, such as trees. If we could re-do our experiment knowing what we
502 know now, we would combine data from natural and transplanted populations to model
503 size-dependent demography over a more realistic size distribution. Other investigators
504 inspired by similar questions about the demographic drivers of range limits should con-

505 sider such a hybrid approach.

506 *Conclusion.* We have documented geographic variation in operational sex ratio; eluci-
507 dated how sex-specific demographic responses to environmental drivers generate this
508 pattern; quantified how female fertility responds to availability of males; and demon-
509 strated that, in the end, sex ratio variation is a rather inconsequential component of
510 declines in population viability at range limits. In Texas bluegrass and, we speculate,
511 other dioecious plants and animals with similar life history and reproductive traits, the
512 geographic distribution is essentially the *female* environmental niche ‘writ large’ (Harg-
513 reaves et al., 2013).

514 Understanding and predicting geographic distributions and their responses to en-
515 vironmental change demands careful consideration of which biological details must be
516 accounted for and which others can be safely ignored. Our results show that complex,
517 non-linear dynamics involving females, males, and frequency-dependent reproduction
518 can be reasonably approximated as a simple, linear process (female-dominant popula-
519 tion growth). We suggest that this is good news. The next challenge is to figure out how
520 often and under what conditions ecologists can get away with it.

521 Acknowledgements

522 We gratefully acknowledge the many individuals who facilitated our field work, es-
523 pecially Dariusz Malinowski, Jason Goldman, Tom Arsuffi, Alan Byboth, John Walker,
524 Kenneth Steigman, Steven Gibson, Wesley Newman, Kerry Griffis, Liz Martin, Melanie
525 Hartman, Brian Northup, Leland Russell, Dexter R Mardis, and Dixie Smith. This work
526 was made possible by a network of biological field stations that hosted our geograph-

527 ically distributed experiment. We acknowledge Sam Houston State University, Texas
528 A&M University, University of Texas, Texas Tech University, Pittsburgh State University,
529 and Wichita State University for investing in field stations and making these facilities
530 available to us. We thank Marion Donald, Kory Kolis, Nakian Kim, and Alex Espana
531 for valuable assistance in the field, lab, and greenhouse. Our work was supported by
532 NSF Division of Environmental Biology awards 1543651 and 1754468 and by the Rice
533 University Faculty Initiatives Fund.

534 **Author contributions**

535 A.C. and T.E.X.M. designed the study, carried out the study, and conducted the statistical
536 analyses. T.E.X.M drafted the manuscript and both authors finalized the submission.

537 **Data accessibility**

538 A data package will be formally published in parallel with this manuscript. For now,
539 reviewers may access our data at <https://github.com/texmiller/POAR-range-limits>.

540 **Literature Cited**

- 541 Araújo, M. S., Bolnick, D. I., and Layman, C. A. (2011). The ecological causes of individ-
542 ual specialisation. *Ecology letters*, 14(9):948–958.
- 543 Bertiller, M. B., Sain, C. L., Bisigato, A. J., Coronato, F. R., Aries, J. O., and Graff, P. (2002).
544 Spatial sex segregation in the dioecious grass *poa ligularis* in northern patagonia: the
545 role of environmental patchiness. *Biodiversity & Conservation*, 11(1):69–84.

- 546 Bialic-Murphy, L., Heckel, C. D., McElderry, R. M., and Kalisz, S. (2020). Deer indi-
547 rectly alter the reproductive strategy and operational sex ratio of an unpalatable forest
548 perennial. *The American Naturalist*, 195(1):56–69.
- 549 Bierzychudek, P. and Eckhart, V. (1988). Spatial segregation of the sexes of dioecious
550 plants. *The American Naturalist*, 132(1):34–43.
- 551 Bisang, I., Ehrlén, J., and Hedenäs, L. (2020). Sex expression and genotypic sex ratio
552 vary with region and environment in the wetland moss *drepanocladus lycopodioides*.
553 *Botanical journal of the Linnean Society*, 192(2):421–434.
- 554 Bolnick, D. I. and Doebeli, M. (2003). Sexual dimorphism and adaptive speciation: two
555 sides of the same ecological coin. *Evolution*, 57(11):2433–2449.
- 556 Bolnick, D. I., Svanbäck, R., Fordyce, J. A., Yang, L. H., Davis, J. M., Hulsey, C. D.,
557 and Forister, M. L. (2002). The ecology of individuals: incidence and implications of
558 individual specialization. *The American Naturalist*, 161(1):1–28.
- 559 Bowyer, R. T. (2004). Sexual segregation in ruminants: definitions, hypotheses, and
560 implications for conservation and management. *Journal of Mammalogy*, 85(6):1039–1052.
- 561 Carpenter, B., Gelman, A., Hoffman, M. D., Lee, D., Goodrich, B., Betancourt, M.,
562 Brubaker, M., Guo, J., Li, P., and Riddell, A. (2017). Stan: A probabilistic program-
563 ming language. *Journal of statistical software*, 76(1).
- 564 Caruso, C. and Case, A. (2007). Sex ratio variation in gynodioecious lobelia siphilit-
565 ica: effects of population size and geographic location. *Journal of Evolutionary Biology*,
566 20(4):1396–1405.

- 567 Caswell, H. (2001). *Matrix Population Models*. Sinauer Associates, Inc., Sunderland, MA,
- 568 2 edition.
- 569 Caswell, H. and Weeks, D. E. (1986). Two-sex models: chaos, extinction, and other
- 570 dynamic consequences of sex. *The American Naturalist*, 128(5):707–735.
- 571 Chen, J., Duan, B., Wang, M., Korpelainen, H., and Li, C. (2014). Intra-and inter-sexual
- 572 competition of *populus cathayana* under different watering regimes. *Functional Ecol-*
- 573 *ogy*, 28(1):124–136.
- 574 Compagnoni, A., Steigman, K., and Miller, T. E. (2017). Can't live with them, can't live
- 575 without them? balancing mating and competition in two-sex populations. *Proceedings*
- 576 *of the Royal Society B: Biological Sciences*, 284(1865):20171999.
- 577 Darwin, C. (1871). *The descent of man*. BoD–Books on Demand.
- 578 De Lisle, S. P., Paiva, S., and Rowe, L. (2018). Habitat partitioning during character
- 579 displacement between the sexes. *Biology letters*, 14(6):20180124.
- 580 De Lisle, S. P. and Rowe, L. (2015). Ecological character displacement between the sexes.
- 581 *The American Naturalist*, 186(6):693–707.
- 582 Diez, J. M., Giladi, I., Warren, R., and Pulliam, H. R. (2014). Probabilistic and spatially
- 583 variable niches inferred from demography. *Journal of ecology*, 102(2):544–554.
- 584 Doak, D. F. and Morris, W. F. (2010). Demographic compensation and tipping points in
- 585 climate-induced range shifts. *Nature*, 467(7318):959–962.
- 586 Dudaniec, R. Y., Carey, A. R., Svensson, E. I., Hansson, B., Yong, C. J., and Lancaster, L. T.

- 587 (2021). Latitudinal clines in sexual selection, sexual size dimorphism, and sex-specific
588 genetic dispersal during a poleward range expansion. *Journal of Animal Ecology*.
- 589 Eberhart-Phillips, L. J., Küpper, C., Miller, T. E., Cruz-López, M., Maher, K. H., Dos Reme-
590 dios, N., Stoffel, M. A., Hoffman, J. I., Krüger, O., and Székely, T. (2017). Sex-specific
591 early survival drives adult sex ratio bias in snowy plovers and impacts mating system
592 and population growth. *Proceedings of the National Academy of Sciences*, 114(27):E5474–
593 E5481.
- 594 Ehrlén, J. and Morris, W. F. (2015). Predicting changes in the distribution and abundance
595 of species under environmental change. *Ecology Letters*, 18(3):303–314.
- 596 Eppley, S. (2001). Gender-specific selection during early life history stages in the dioe-
597 cious grass *distichlis spicata*. *Ecology*, 82(7):2022–2031.
- 598 Eppley, S. M. (2006). Females make tough neighbors: sex-specific competitive effects in
599 seedlings of a dioecious grass. *Oecologia*, 146(4):549–554.
- 600 Evans, M. E., Merow, C., Record, S., McMahon, S. M., and Enquist, B. J. (2016). To-
601 wards process-based range modeling of many species. *Trends in Ecology & Evolution*,
602 31(11):860–871.
- 603 Ewen, J. G., Thorogood, R., and Armstrong, D. P. (2011). Demographic consequences of
604 adult sex ratio in a reintroduced hihi population. *Journal of Animal Ecology*, 80(2):448–
605 455.
- 606 Fick, S. E. and Hijmans, R. J. (2017). Worldclim 2: new 1-km spatial resolution climate
607 surfaces for global land areas. *International journal of climatology*, 37(12):4302–4315.

- 608 Field, D. L., Pickup, M., and Barrett, S. C. (2013a). Comparative analyses of sex-ratio vari-
609 ation in dioecious flowering plants. *Evolution: International Journal of Organic Evolution*,
610 67(3):661–672.
- 611 Field, D. L., Pickup, M., and Barrett, S. C. (2013b). Ecological context and metapopula-
612 tion dynamics affect sex-ratio variation among dioecious plant populations. *Annals of*
613 *botany*, 111(5):917–923.
- 614 Franco, M. and Silvertown, J. (2004). A comparative demography of plants based upon
615 elasticities of vital rates. *Ecology*, 85(2):531–538.
- 616 Gelman, A., Meng, X.-L., and Stern, H. (1996). Posterior predictive assessment of model
617 fitness via realized discrepancies. *Statistica sinica*, pages 733–760.
- 618 Gianuca, D., Votier, S. C., Pardo, D., Wood, A. G., Sherley, R. B., Ireland, L., Choquet,
619 R., Pradel, R., Townley, S., Forcada, J., et al. (2019). Sex-specific effects of fisheries and
620 climate on the demography of sexually dimorphic seabirds. *Journal of Animal Ecology*.
- 621 Gownaris, N. J., García Borboroglu, P., and Boersma, P. D. (2020). Sex ratio is vari-
622 able and increasingly male biased at two colonies of magellanic penguins. *Ecology*,
623 101(3):e02939.
- 624 Groen, K. E., Stieha, C. R., Crowley, P. H., and McLetchie, D. N. (2010). Sex-specific plant
625 responses to light intensity and canopy openness: implications for spatial segregation
626 of the sexes. *Oecologia*, 162(3):561–570.
- 627 Hargreaves, A. L., Samis, K. E., and Eckert, C. G. (2013). Are species' range limits simply
628 niche limits writ large? a review of transplant experiments beyond the range. *The*
629 *American Naturalist*, 183(2):157–173.

- 630 Holt, R. D. (2009). Bringing the hutchinsonian niche into the 21st century: ecological and
631 evolutionary perspectives. *Proceedings of the National Academy of Sciences*, 106(Supple-
632 ment 2):19659–19665.
- 633 Hultine, K. R., Bush, S. E., Ward, J. K., and Dawson, T. E. (2018). Does sexual dimorphism
634 predispose dioecious riparian trees to sex ratio imbalances under climate change? *Oe-
635 cologia*, 187(4):921–931.
- 636 Hutchinson, G. E. (1958). Concluding remarks. In *Cold Spring Harbour Symposium on
637 Quantitative Biology*, volume 22, pages 415—427.
- 638 Ketterson, E. D. and Nolan Jr, V. (1976). Geographic variation and its climatic correlates in
639 the sex ratio of eastern-wintering dark-eyed juncos (*junco hyemalis hyemalis*). *Ecology*,
640 57(4):679–693.
- 641 Law, C. J. and Mehta, R. S. (2018). Carnivory maintains cranial dimorphism between
642 males and females: evidence for niche divergence in extant musteloidea. *Evolution*,
643 72(9):1950–1961.
- 644 Lee-Yaw, J. A., Kharouba, H. M., Bontrager, M., Mahony, C., Csergő, A. M., Noreen,
645 A. M., Li, Q., Schuster, R., and Angert, A. L. (2016). A synthesis of transplant exper-
646 iments and ecological niche models suggests that range limits are often niche limits.
647 *Ecology letters*, 19(6):710–722.
- 648 Louthan, A. M., Doak, D. F., and Angert, A. L. (2015). Where and when do species
649 interactions set range limits? *Trends in Ecology & Evolution*, 30(12):780–792.
- 650 Lynch, H. J., Rhainds, M., Calabrese, J. M., Cantrell, S., Cosner, C., and Fagan, W. F.

- 651 (2014). How climate extremes-not means-define a species' geographic range boundary
652 via a demographic tipping point. *Ecological Monographs*, 84(1):131–149.
- 653 Merow, C., Bois, S. T., Allen, J. M., Xie, Y., and Silander, J. A. (2017). Climate change both
654 facilitates and inhibits invasive plant ranges in new england. *Proceedings of the National
655 Academy of Sciences*, 114(16):E3276–E3284.
- 656 Merow, C., Latimer, A. M., Wilson, A. M., McMahon, S. M., Rebelo, A. G., and Silander Jr,
657 J. A. (2014). On using integral projection models to generate demographically driven
658 predictions of species' distributions: development and validation using sparse data.
659 *Ecography*, 37(12):1167–1183.
- 660 Miller, T. E. and Inouye, B. D. (2011). Confronting two-sex demographic models with
661 data. *Ecology*, 92(11):2141–2151.
- 662 Miller, T. E. and Inouye, B. D. (2013). Sex and stochasticity affect range expansion of
663 experimental invasions. *Ecology Letters*, 16(3):354–361.
- 664 Miller, T. E., Shaw, A. K., Inouye, B. D., and Neubert, M. G. (2011). Sex-biased dispersal
665 and the speed of two-sex invasions. *The American Naturalist*, 177(5):549–561.
- 666 Milner-Gulland, E., Bukreeva, O., Coulson, T., Lushchekina, A., Kholodova, M., Bekenov,
667 A., and Grachev, I. A. (2003). Reproductive collapse in saiga antelope harems. *Nature*,
668 422(6928):135–135.
- 669 Mysterud, A., Coulson, T., and Stenseth, N. C. (2002). The role of males in the dynamics
670 of ungulate populations. *Journal of Animal Ecology*, 71(6):907–915.
- 671 Pekár, S., Martišová, M., and Bilde, T. (2011). Intersexual trophic niche partitioning in an
672 ant-eating spider (araneae: Zodariidae). *PloS one*, 6(1):e14603.

- 673 Petry, W. K., Soule, J. D., Iler, A. M., Chicas-Mosier, A., Inouye, D. W., Miller, T. E.,
674 and Mooney, K. A. (2016). Sex-specific responses to climate change in plants alter
675 population sex ratio and performance. *Science*, 353(6294):69–71.
- 676 Phillips, R., Silk, J., Phalan, B., Catry, P., and Croxall, J. (2004). Seasonal sexual segre-
677 gation in two thalassarche albatross species: competitive exclusion, reproductive role
678 specialization or foraging niche divergence? *Proceedings of the Royal Society of London.*
679 *Series B: Biological Sciences*, 271(1545):1283–1291.
- 680 Rankin, D. J. and Kokko, H. (2007). Do males matter? the role of males in population
681 dynamics. *Oikos*, 116(2):335–348.
- 682 Renganayaki, K., Jessup, R., Burson, B., Hussey, M., and Read, J. (2005). Identification of
683 male-specific afp markers in dioecious texas bluegrass. *Crop science*, 45(6):2529–2539.
- 684 Renganayaki, K., Read, J., and Fritz, A. (2001). Genetic diversity among texas bluegrass
685 genotypes (poa arachnifera torr.) revealed by afp and rapd markers. *Theoretical and*
686 *Applied Genetics*, 102(6-7):1037–1045.
- 687 Renner, S. S. and Ricklefs, R. E. (1995). Dioecy and its correlates in the flowering plants.
688 *American journal of botany*, 82(5):596–606.
- 689 Rozas, V., DeSoto, L., and Olano, J. M. (2009). Sex-specific, age-dependent sensitivity of
690 tree-ring growth to climate in the dioecious tree juniperus thurifera. *New Phytologist*,
691 182(3):687–697.
- 692 Shelton, A. O. (2010). The origin of female-biased sex ratios in intertidal seagrasses
693 (phyllospadix spp.). *Ecology*, 91(5):1380–1390.

- 694 Sheth, S. N. and Angert, A. L. (2018). Demographic compensation does not rescue
695 populations at a trailing range edge. *Proceedings of the National Academy of Sciences*,
696 115(10):2413–2418.
- 697 Shine, R. (1989). Ecological causes for the evolution of sexual dimorphism: a review of
698 the evidence. *The Quarterly Review of Biology*, 64(4):419–461.
- 699 Stan Development Team (2020). RStan: the R interface to Stan. R package version 2.21.2.
- 700 Temeles, E. J., Miller, J. S., and Rifkin, J. L. (2010). Evolution of sexual dimorphism
701 in bill size and shape of hermit hummingbirds (phaethornithinae): a role for eco-
702 logical causation. *Philosophical Transactions of the Royal Society B: Biological Sciences*,
703 365(1543):1053–1063.
- 704 Veran, S. and Beissinger, S. R. (2009). Demographic origins of skewed operational and
705 adult sex ratios: perturbation analyses of two-sex models. *Ecology Letters*, 12(2):129–
706 143.
- 707 Villegas, J., Doak, D. F., García, M. B., and Morris, W. F. (2015). Demographic compen-
708 sation among populations: what is it, how does it arise and what are its implications?
709 *Ecology letters*, 18(11):1139–1152.
- 710 Wood, S. (2017). *Generalized Additive Models: An Introduction with R*. Chapman and
711 Hall/CRC, 2 edition.

Appendix A: Site locations and climate

	Population	Latitude	Longitude	Year_visited	Experimental_source
1	Canyon_of_Eagles	30.88	-98.43	2012	no
2	ClearBay-Thunderbird	35.23	-97.24	2013	no
3	CooperWMA	36.60	-99.51	2012	yes
4	Copper Breaks	34.10	-99.75	2013	yes
5	Dinosaur_Valley	32.25	-97.82	2012	no
6	Fort_Worth_Nature_Center	32.83	-97.46	2012	no
7	Ft Cobb	35.18	-98.45	2013	no
8	Ft Richardson	33.20	-98.16	2013	no
9	Great Plains	34.74	-98.97	2013	no
10	Great_Salt_Plains	36.79	-98.18	2012	no
11	Horn_Hill_Cemetery	31.56	-96.64	2012	yes
12	Kingman_Fishing_Lake	37.65	-98.28	2012	no
13	Lake Arrowhead	33.75	-98.39	2013	yes
14	Mineral_Wells	32.89	-98.01	2012	no
15	Pedernales_Falls	30.33	-98.25	2012	no
16	Possum Kingdom	32.87	-98.57	2013	no
17	Quartz_Mountain	34.89	-99.30	2012	yes
18	Red Rock Canyon	35.44	-98.35	2013	no
19	Red_River	34.13	-98.10	2012	no
20	South_Llano	30.45	-99.80	2012	yes
21	Sulfur_Springs	31.08	-98.46	2012	yes
22	Wichita_Mountains	34.70	-98.67	2012	no

Table A1: Sites of natural population surveys

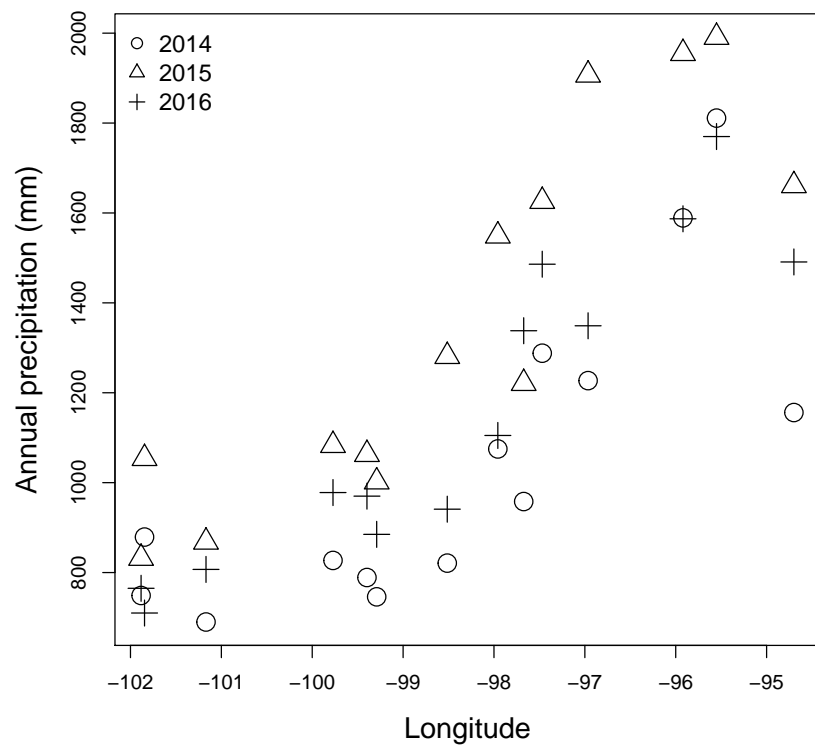


Figure A1: Total annual precipitation at common garden sites during the study years tracked long-term trends of increasing aridity from east to west.

Appendix B: Additional results

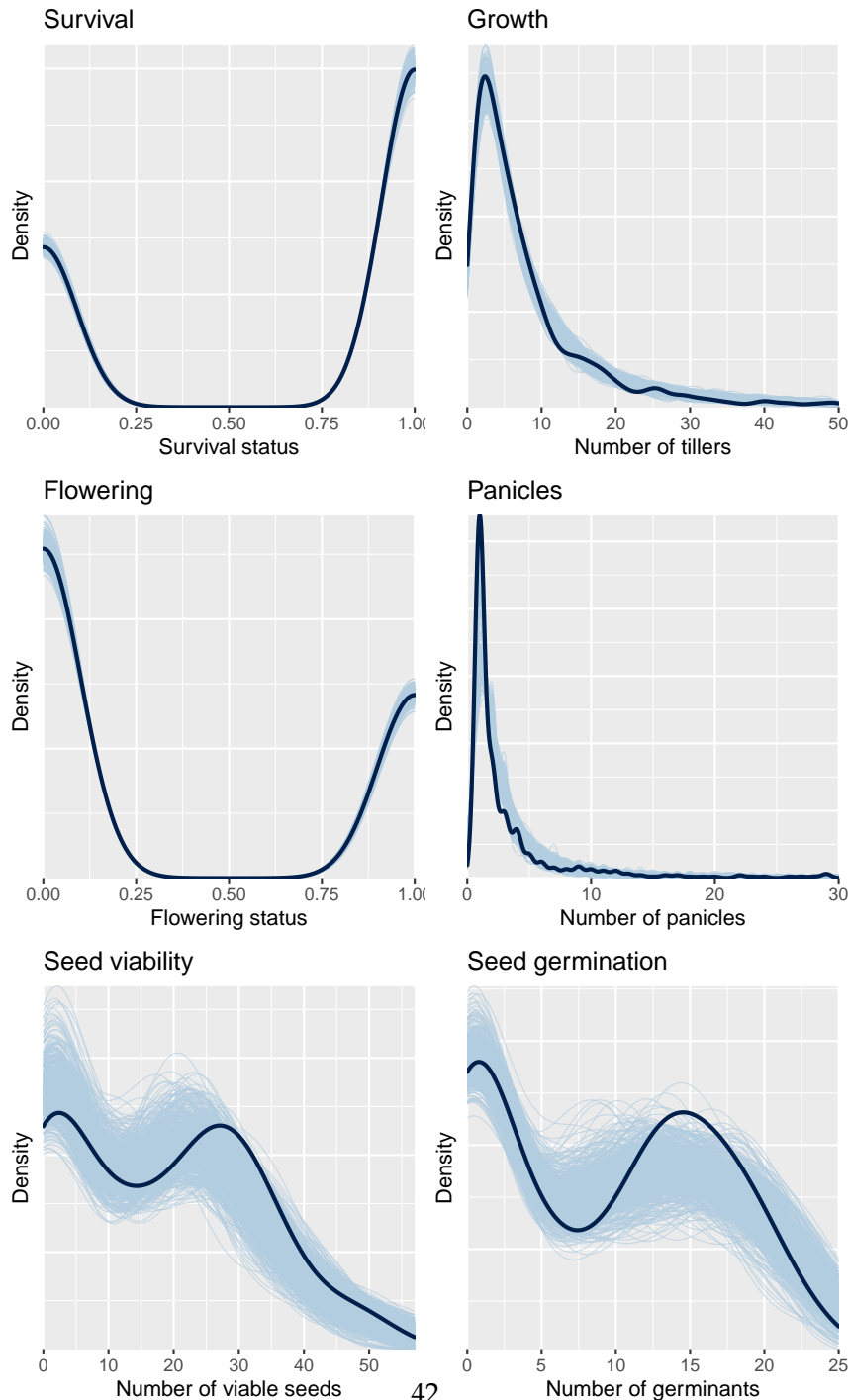


Figure B1: Posterior predictive checks of statistical models for demographic vital rates. Lines show density distributions of real data (thick, dark blue) compared to simulated data sets (thin, light blue) generated from the fitted models based on 500 draws of the posterior distribution of parameter estimates. Correspondence of the real and simulated data suggests that the fitted models describe the data well.

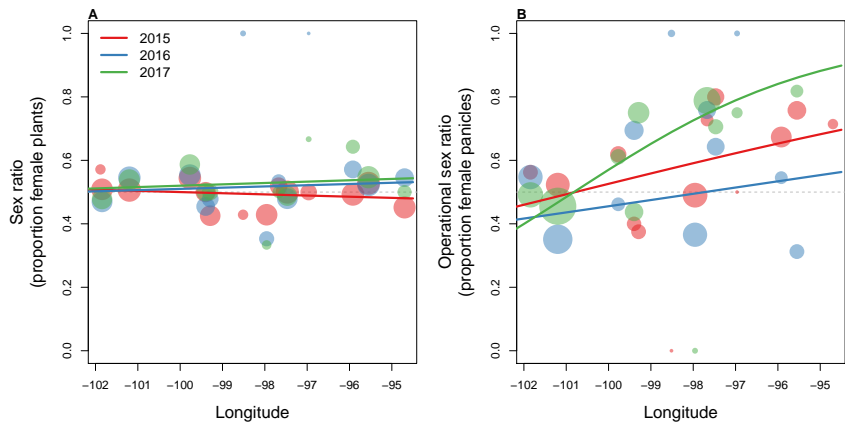


Figure B2: Year-specific sex ratios of plants (A) and panicles (B) in common garden populations spanning the longitudinal aridity gradient. Points sizes are proportional to sample sizes and lines show fitted binomial GLMs.

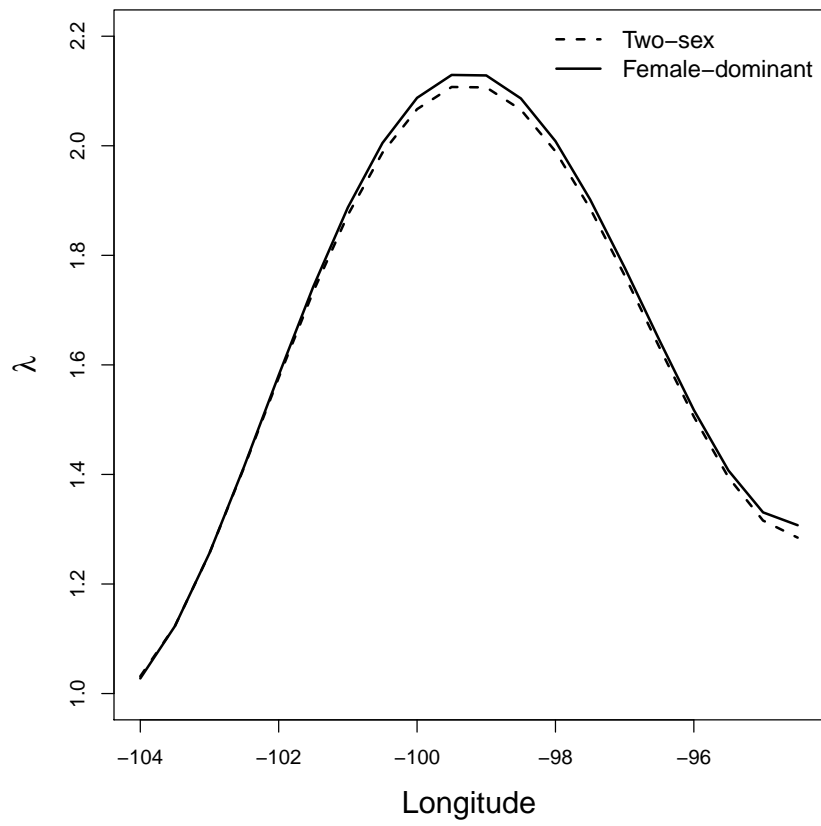


Figure B3: Comparison of longitudinal variation in λ between the two-sex demographic model (dashed line) that includes dependence of female seed production on population structure and the corresponding female-dominant model (solid line) with constant female fertility and all else equal. Models were evaluated at posterior mean parameter estimates

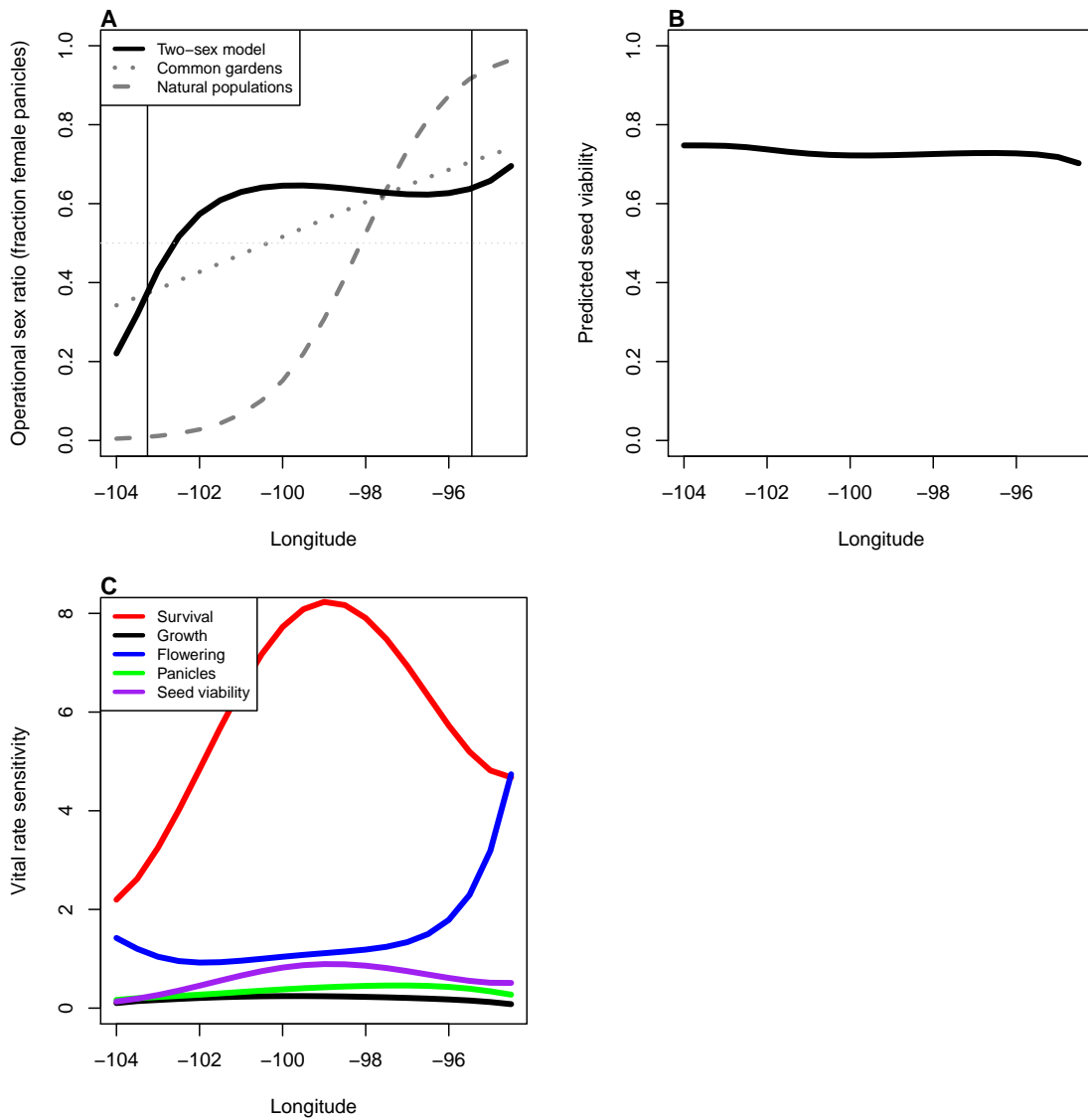


Figure B4: **A**, Longitudinal variation in operational sex ratio (fraction of panicles that are female) predicted by the two-sex MPM (solid line) compared to the sex ratio clines fitted to data from common gardens (dotted line) or natural populations (dashed line). Vertical lines show the longitudes of the westernmost and easternmost counties with occurrence records of *P. arachnifera*. **B**, Longitudinal variation in seed viability predicted by the two-sex MPM according to Eq. 1 and the OSR variation shown in **A**. **C**, Sensitivities of λ to vital rates in relation to longitude. Sensitivities were calculated numerically by perturbing vital rate functions (across all sizes) by 0.01, recalculating λ , and dividing the difference by 0.01. Vital rates were perturbed equally for both sexes though results in Fig 6B,C suggest that vital rate sensitivities were dominated by females.

714 **Appendix C: Size distribution comparisons and simulation
715 experiments**

716 In this section, we compare size distributions of natural and experimental populations,
717 and explore how the size distribution predicted by the two-sex MPM affects our conclu-
718 sions about the role of males in range boundary formation.

719 *Observed and predicted size distributions*

720 *Natural populations.* During natural population surveys (2012–2013) we recorded the
721 area (m^2) of Texas bluegrass patches using a Trimble GeoExplorer hand-held GPS re-
722 ceiever with sub-meter accuracy.

723 *Common garden populations.* Common garden data collection included tiller counts and
724 the maximum length and width of each patch, which we converted to area (m^2) assuming
725 an oval shape. We used these data to estimate the relationship between patch area and
726 tiller count (Fig. C1) using a generalized additive model (Wood, 2017) and applied this
727 fitted relationship to area measurements from natural populations. This allowed us to
728 compare the size distributions of natural and common garden populations (pooled across
729 the range) in the same size unit ($\log(\text{tillers})$).

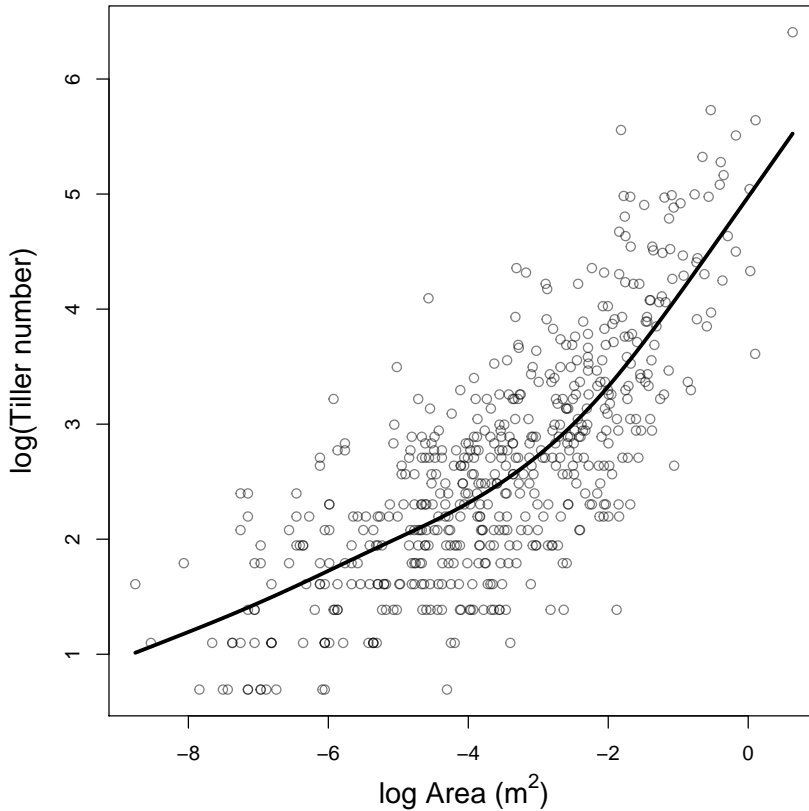


Figure C1: Relationship between area (m^2) and tiller count from plants in the common garden experiment. The fitted gam model (line) was used to convert area measurements from natural populations to tiller counts.

730 Two-sex MPM. The two-sex MPM predicts asymptotic population structure, including
 731 stable size distribution (SSD) and sex ratio. For comparison with empirical data, we
 732 calculated the SSD (pooling both sexes) predicted in the center of the range (the conclu-
 733 sions that we draw from this analysis hold up if we consider SSD from different parts
 734 of the range). Because the MPM is structured by tiller number, we converted the SSD to
 735 log(tillers) by simulating an arbitrarily large (10000) population at SSD, taking the natural

⁷³⁶ logarithm of tiller number, and then estimating the empirical distribution of this variable.

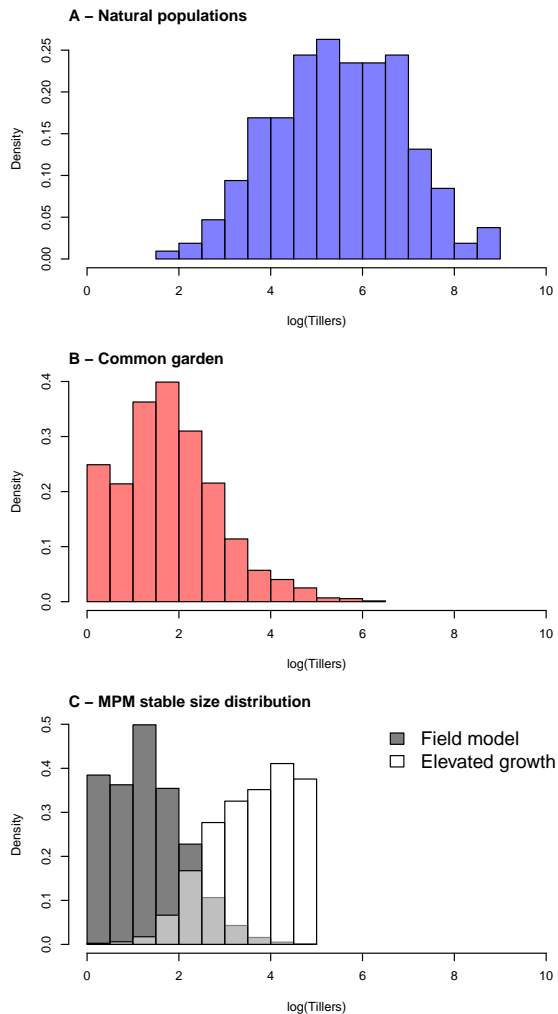


Figure C2: Size distribution of Texas bluegrass from natural populations (A), common garden populations (B), and predicted by the two-sex MPM (C). In C, the two size distributions come from the base model parameterized following methods described in the main manuscript (“field model”, in gray) and a numerical experiment where growth parameters were numerically increased to generate a size distribution more consistent with natural populations (“elevated growth model”, in white).

737 *Results.* Plants from natural populations were larger, on average, than plants in our
 738 common garden experiment (Fig. C2A,B). Common garden plants were generally larger

739 each year but the largest sizes in the final year of the common garden corresponded
740 to smaller sizes observed in natural populations (although natural population surveys
741 were subject to detection bias: small plants were likely under-sampled relative to their
742 occurrence). The predicted SSD from the two-sex MPM was consistent with the common
743 garden size distribution (Fig. C2C), as expected since the model was built with common
744 garden data. These results suggest that common garden plants did not have the same
745 growth trajectories of naturally occurring plants and / or were not given sufficient time
746 to reach the sizes observed in natural populations.

747 *Numerical experiment to explore the consequences of under-estimating
748 the size distribution*

749 The preceding results indicate that the common garden populations, and thus the two-
750 sex MPM built from common garden data, under-estimate the size distribution of Texas
751 bluegrass, relative to what we find in natural populations. Sex differences in demog-
752 raphy, and especially flowering, were most pronounced for the largest sizes (Fig. 4),
753 but these sizes were predicted to be very rare in a stable population (Fig. C2C). The
754 under-estimation of large sizes may explain why longitudinal clines in OSR predicted
755 by the MPM and seen in the common garden were weaker than the OSR cline observed
756 in natural populations (Fig. B4). It is therefore possible that our main finding – that
757 males contribute little-to-nothing toward range limitation – reflects a limitation of the
758 model, since real populations tended to be more female-biased (and potentially more
759 mate-limited) in the eastern range margins than the model predicted. To explore this
760 possibility, we conducted a numerical experiment that allowed modeled plants to reach
761 larger sizes by increasing the empirically-estimated intercept of the growth vital rate

762 function by a factor of 2.75 (values larger than this caused numerical instabilities). This
763 adjustment caused all plants to increase in size more strongly regardless of initial size,
764 sex, or geographic location. We also increased the upper size limit to $U * 1.5$.

765 As expected, this led to stronger sex ratio clines and stronger reductions in seed vi-
766 ability at eastern range margins (Fig. C3). These changes increased the contributions of
767 males to eastern range limitation in the elevated-growth numerical experiment. How-
768 ever, the contribution of males to range limitation was still weak relative to that of females
769 (the maximum male contribution was less than half of the female maximum) and differ-
770 ences between the two-sex and female-dominant MPMs were still very minor (Fig. C4).
771 Collectively, these results suggest that the small size distribution of the common garden
772 experiment led to a weaker role of males than would be expected in populations with a
773 more realistic size distribution, but that even with a larger size distribution, declines in
774 female performance still dominate range boundary formation.

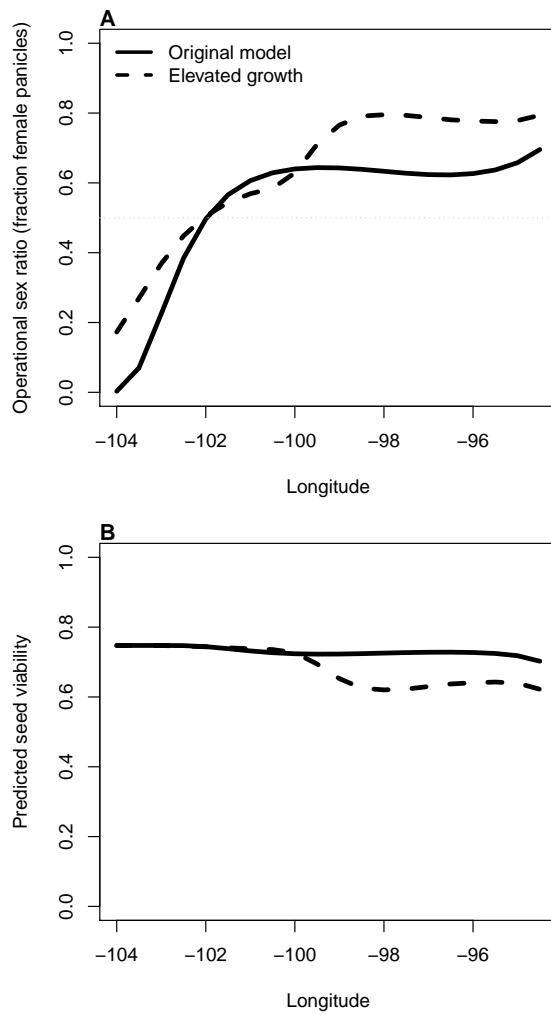


Figure C3: Two-sex model predictions for **A** operational sex ratio (fraction of panicles that are female) and **B** seed viability at stable population structure in relation to longitude. Solid line shows predictions of the base model using field-estimated parameter values and dashed line shows the same model with elevated growth of both sexes and across all longitudes (intercept of growth function increased by a factor of 2.75).

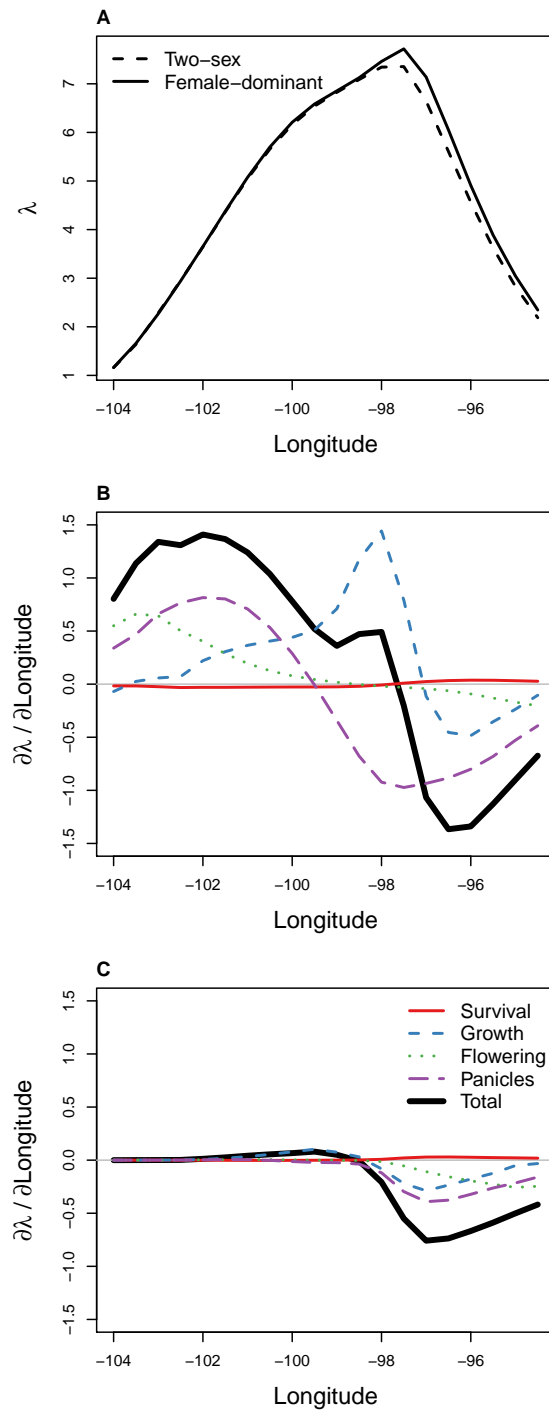


Figure C4: Results for the elevated growth model, in which the intercept of growth function was increased by a factor of 2.75. **A**, contrast of two-sex and female-dominant models, as in Fig. B3; **B,C**, Life Table Response Experiments decomposing the change in λ with respect to longitude into contributions from female **B** and male **C** vital rates (layout as in Fig. 6).

Site		City, State	Latitude	Longitude
1	Buffalo Lake National Wildlife Refuge	Amarillo, TX	35.20	-101.85
2	USDA-ARS Grazinglands Research Laboratory	El Reno, OK	35.53	-97.96
3	Katy Prairie Conservatory Indiangrass Preserve	Waller, TX	29.92	-95.92
4	Texas Tech University Llano River Research Station	Junction, TX	30.49	-99.77
5	Lake Lewisville Environmental Learning Area	Lewisville, TX	33.07	-96.96
6	University of Texas Stengl Lost Pines Biological Station	Bastrop, TX	30.18	-97.47
7	Texas Tech University	Lubbock, TX	33.57	-101.88
8	Wichita State University Ninnescah Field Station	Wichita, KS	37.54	-97.67
9	Texas A&M AgriLife Research and Extension Center	Ozona, TX	30.71	-101.20
10	Pittsburgh State University Field Station	Pittsburgh, KS	37.41	-94.70
11	Sam Houston State University Center for Biological Field Studies	Huntsville, TX	30.72	-95.55
12	Texas A&M AgriLife Research and Extension Center	Vernon, TX	34.15	-99.29
13	River Bend Nature Center	Wichita Falls, TX	33.91	-98.51
14	USDA-ARS Range and Pasture Research	Woodward, OK	36.43	-99.40

Table A2: Sites of common garden experiments